Nuclear Energy Agency

NEA/NSC/R(2020)8

Unclassified

English text only

28 January 2022

NUCLEAR ENERGY AGENCY
NUCLEAR SCIENCE COMMITTEE

# Subgroup 27: Prompt Photon Production from Fission Products

This document is available in PDF format only.

JT03488744

# *Foreword*

Designing and operating nuclear energy facilities requires knowledge of fundamental nuclear physics. That in turn requires data on interaction probabilities between incident particles, particle emission probabilities and much more.

The Nuclear Energy Agency (NEA) Working Party on International Nuclear Data Evaluation Co-operation (WPEC) was established under the NEA Nuclear Science Committee (NSC) in 1989 to promote the exchange of information on nuclear data. Following the recommendations of the WPEC Subgroup 21 on the "Assessment of neutron cross-section evaluations for the bulk of fission products" and the subsequent WPEC Subgroup 23 that worked on an "Evaluated data library for the bulk of the fission products", WPEC launched Subgroup 27 to investigate the gamma source information on fission product nuclides.

The following report is issued by the WPEC Subgroup 27, which builds upon the work of the previous Subgroups 21 and 23, critically reviewing the gamma emission data and providing recommendations to improve nuclear data libraries around the world.

# *Acknowledgements*

The NEA wishes to express its sincere gratitude to Dr Robert Jacqmin (France), who co-ordinated this report and the WPEC Subgroup 27 activities, to the members of Subgroup 27 and to the authors for their contribution to this report.

Special thanks are also due to Dr Christopher Dean (United Kingdom), who passed away in 2012 and who was the principal author of a large body of work within Subgroup 27.

# *Table of contents*

# *List of abbreviations and acronyms*

| | |
|---|---|
| AGR | Advanced gas-cooled reactor |
| BNL | Brookhaven National Laboratory (United States) |
| CASTHY | Nuclear statistical model calculation code (Japan) |
| CEA | Commissariat à l'énergie atomique (France) |
| CERN | Conseil européen pour la recherche nucléaire |
| CRP | Co-ordinated Research Project (IAEA) |
| DANCE | Detector for advanced neutron capture experiments (LANL, United States) |
| DICEBOX | Monte Carlo code for the simulation of gamma decay |
| EAF | European activation file |
| EGAF | Evaluated Gamma-ray Activation File |
| EMPIRE | Nuclear reaction code (United States) |
| ENDF | Evaluated Nuclear Data File (United States) |
| ENDF-6 | Evaluated Nuclear Data File Format version 6 |
| ENSDF | Evaluated Nuclear Structure Data File |
| EOLE | Zero-power nuclear reactor (CEA, France) |
| eV | Electronvolt (unit of energy) |
| EXFOR | EXchange FORmat |
| GIF | Generation IV |
| GROUPR | Module of the NJOY code responsible for generating multi-group data |
| HEATR | Module of the NJOY code responsible for heating and radiation damage processing |
| IAEA | International Atomic Energy Agency |
| JANIS | JAva-based Nuclear Data Information System (NEA) |
| JEFF | Joint Evaluated Fission and Fusion File (NEA) |
| JENDL | Japanese Evaluated Nuclear Data Library |
| JHR | Jules Horowitz Reactor |
| KERMA | Kinetic energy released per unit mass |
| LANL | Los Alamos National Laboratory (United States) |
| LWR | Light water reactor |

| | |
|---|---|
| MeV | Milli-electronvolt (unit of energy) |
| MF | File data block within the ENDF format |
| MOX | Mixed oxide fuel |
| MT | Reaction data block within the ENDF format |
| NEA | Nuclear Energy Agency |
| NJOY | Nuclear data processing code (LANL, United States) |
| NNDC | National Nuclear Data Center (United States) |
| NSC | Nuclear Science Committee (NEA) |
| PGAA | Prompt Gamma Activation Analysis |
| PWR | Pressurised water reactor |
| RIPL | Reference Input Parameter Library |
| TALYS | Nuclear reaction code (European Union) |
| TENDL | TALYS-based Evaluated Nuclear Data Library (European Union) |
| TOF | Time of flight measurement technique |
| TRIPOLI | Monte Carlo radiation transport code (CEA, France) |
| WIMS | Winfrith Improved Multi-group Scheme (United Kingdom) |
| WPEC | Working Party on International Nuclear Data Evaluation Co-operation (NEA) |

# *Executive summary*

Knowledge of basic nuclear physics is fundamental to our ability to model, simulate and understand the operation of nuclear systems. State-of-the-art databases in this field contain uncertainties that reflect those of the experiments they are based on. These uncertainties result in more conservative approaches, particularly for advanced reactor designs and fuel cycles. Identifying the priorities for new nuclear physics measurements has always been a key objective of the Nuclear Energy Agency (NEA) Working Party on International Nuclear Data Evaluation Co-operation (WPEC).

Fission creates two residual nuclei that are neutron-rich and unstable, hence the physics of their interaction with radiation is relatively poorly known. Following other WPEC subgroups that assessed neutron interactions with fission products, this subgroup addressed the production of gamma radiation through nuclear reaction, which is essential in the understanding of heating in non-fissile materials within a reactor.

A rigorous prioritisation exercise was carried out to identify isotopes of importance and this was followed by a review of the experimental measurements, evaluated files and processed data relevant to gamma production in these isotopes. In-depth studies were carried out for specific isotopes and data sets. From these analyses, a range of recommendations are made for improvements in data evaluation methodology and priority isotopes for re-evaluation in major nuclear data libraries. Work on the re-evaluation of gamma spectra for a set of stable isotopes of importance to nuclear energy technology is reviewed before the main conclusions are drawn.

# 1. Introduction

In a typical nuclear reactor, some 10-12% of heating comes from the energy deposited by gamma rays. The major photon production sources (in equal proportions) include prompt neutron induced fission, capture of prompt neutrons and the decay of fission plus activation daughter products. The photons penetrate some distance from their birth and can cause some 80-90% of heating in non-fissile regions. Without some actions, this could lead to distortion of control rods and chemical damage in moderators, e.g. enhancing graphite erosion rate.

There is considerable interest in extending fuel life (deep burn) and this in turn leads to an increased inventory of higher actinides and more fission products (nuclides with Z=35-70). A survey in 2003 of the Joint Evaluated Fission and Fusion File (JEFF-3.0), Evaluated Nuclear Data File (ENDF/B-VI.8) and Japanese Evaluated Nuclear Data Library (JENDL-3.3) nuclear data libraries indicated that few modern evaluations in the mass range of fission products contained gamma source data. Where data were present, they were often old and incomplete.

The Working Party on International Nuclear Data Evaluation Co-operation (WPEC) operates through the creation of subgroups that focus on the different evaluated data groups worldwide to collaborate on matters of common interest.

In 2006, WPEC accepted a proposal for Subgroup 27 "to make recommendations on prompt photon production data for fission product nuclei". The purpose of these data is to be added to the most relevant general-purpose evaluations, including the evaluations assembled by the WPEC Subgroup 23 (NEA, 2009) following the review by the WPEC Subgroup 21 (NEA, 2005). While some of these evaluations include gamma source data, most do not.

This document assesses available gamma source data and describes potential difficulties associated with choices. It starts with a discussion of prioritisation.

# 2. Prioritisation of reaction data

Fission products are important neutron absorbers in fuel at the end of life in thermal and fast reactors. They are rather heavy isotopes to be of major interest to the nuclear fusion community, which has often used separate activation data such as the European activation file (EAF). Fast reactors are generally considered a future development (e.g. all but one of the systems considered by the Generation IV Forum [GIF] are fast reactors) so the major current interest in fission products for operational reactors is as thermal absorbers.

The neutron spectrum in the fuel of thermal reactors peaks at energies below one electronvolt (eV). Unless the neutron capture,[1] (n,γ), cross-section is extremely small (in which case it is not important), neutron absorption rates in fission products can typically be approximated to be the same as (n,γ) rates.

The WPEC Subgroup 27 limited its studies to gamma sources from (n,γ) reaction at thermal and low resonance energies below a few keV. Here, the energy release can be taken as the Q value in the evaluations, equivalent to the neutron separation energy for the compound nucleus. The energy of the neutron can be virtually ignored when considering the gamma rays emitted.

Many different fission products result from fission. Those with significant half-lives remain in the fuel to absorb neutrons and emit gamma radiation. The importance of the gamma radiation source is directly related to the size of the absorption cross-sections, but also the quantity generated and the neutron energy spectrum.

Some 89 important fission products are modelled in the Winfrith Improved Multi-group Scheme (WIMS) code (Newton et al., 2008) as part of this work. To obtain this list (Webster, 1995), Webster modelled pressurised water reactor (PWR) and advanced gas-cooled reactor (AGR) uranium oxide ($UO_2$) and mixed oxide (MOX) fuels to calculate reactivity worth values. Isotopic components were then organised by their relative reactivity contributions until 99% of reactivity worth was accounted for in all scenarios. For typical PWR UOX fuel irradiated to 60 GWd/te over 4 years, $^{135}Xe$ contributes approximately 10% of reactivity, the next largest nine isotopic components contribute approximately 50% and the next 15 largest isotopic components contribute approximately 40%.

Table 1 incorporates a mass ordered list of the WIMS fission products, together with their ranking (noting that position 68 marks the 99$^{th}$ percentile on worth for the above PWR case).

1. The symbols here are interpreted as a pair of incident and outgoing particle(s), so that (n,γ) means that an incident neutron reacts and no hadronic material is ejected – only prompt gamma radiation.

**Table 1. Sources of capture gamma source data**

| Isotope | Rank | JEFF-3.1 | ENDF/B-VII.0 | JENDL-3.3 | BNL Data | IAEA Data* |
|---|---|---|---|---|---|---|
| 36Kr83 | 34 | NO | NO | NO | YES | YES |
| 39Y89 | >68 | 12 | 6 | NO | YES | YES |
| 40Zr91 | 50 | 12 | 12 | 12 | YES | YES |
| 40Zr93 | 24 | NO | NO | NO | NO | NO |
| 40Zr95 | >68 | NO | NO | NO | NO | NO |
| 40Zr96 | 47 | 12 | 12 | 12 | NO | YES |
| 41Nb95 | 67 | NO | NO | NO | NO | NO |
| 42Mo95 | 17 | 6 | 6 | 12 | YES | YES |
| 42Mo96 | 68 | 12 | 12 | 12 | YES | YES |
| 42Mo97 | 33 | 12 | 12 | 12 | YES | YES |
| 42Mo98 | 37 | 12 | NO | 12 | YES | YES |
| 42Mo100 | 48 | NO | NO | 12 | YES | YES |
| 43Tc99 | 6 | 6 | 6 | NO | YES | NO |
| 44Ru100 | 52 | 6 | NO | NO | YES | YES |
| 44Ru101 | 18 | NO | 6 | NO | NO | YES |
| 44Ru102 | 45 | NO | NO | NO | YES | YES |
| 44Ru103 | 29 | NO | NO | NO | NO | NO |
| 44Ru104 | 44 | NO | NO | NO | YES | YES |
| 44Ru105 | >68 | NO | NO | NO | NO | NO |
| 45Rh103 | 2 | NO | 6 | NO | YES | YES |
| 45Rh105 | 28 | NO | NO | NO | NO | NO |
| 46Pd104 | 41 | NO | 12 | NO | NO | YES |
| 46Pd105 | 19 | NO | 6 | NO | YES | YES |
| 46Pd106 | 59 | NO | 12 | NO | NO | YES |
| 46Pd107 | 23 | NO | NO | NO | NO | NO |
| 46Pd108 | 22 | NO | 12 | NO | YES | YES |
| 47Ag109 | 15 | NO | 6 | 12 | YES | YES |
| 48Cd110 | 49 | NO | NO | 12 | YES | YES |
| 48Cd111 | 61 | NO | 12 | 12 | YES | YES |
| 48Cd113 | 42 | NO | NO | 12 | YES | YES |
| 49In115 | 54 | NO | NO | NO | YES | YES |
| 53I127 | 43 | NO | 12 | NO | YES | YES |
| 53I129 | 36 | NO | NO | NO | YES | NO |
| 53I131 | >68 | NO | NO | NO | NO | NO |
| 53I135 | >68 | NO | NO | NO | NO | NO |
| 54Xe128 | >68 | NO | NO | NO | NO | YES |
| 54Xe129 | >68 | NO | NO | NO | YES | YES |

**Table 1. Sources of capture gamma source data (Continued)**

| Isotope | Rank | JEFF-3.1 | ENDF/B-VII.0 | JENDL-3.3 | BNL Data | IAEA Data* |
|---|---|---|---|---|---|---|
| 54Xe130 | >68 | NO | NO | NO | NO | YES |
| 54Xe131 | 5 | NO | 6 | NO | YES | YES |
| 54Xe132 | 58 | NO | NO | NO | NO | NO |
| 54Xe133 | 55 | NO | NO | NO | NO | NO |
| 54Xe134 | >68 | NO | NO | NO | NO | NO |
| 54Xe135 | 1 | NO | NO | NO | NO | NO |
| 54Xe136 | >68 | NO | NO | NO | YES | YES |
| 55Cs133 | 3 | NO | 6 | NO | YES | YES |
| 55Cs134 | 20 | NO | NO | NO | YES | NO |
| 55Cs135 | 30 | NO | NO | NO | NO | NO |
| 55Cs137 | >68 | NO | NO | NO | NO | NO |
| 56Ba134 | 64 | NO | NO | NO | YES | YES |
| 57La139 | 31 | NO | NO | NO | YES | YES |
| 58Ce141 | 46 | NO | NO | NO | NO | NO |
| 58Ce142 | 65 | NO | NO | NO | YES | YES |
| 58Ce144 | >68 | NO | NO | NO | NO | NO |
| 59Pr141 | 25 | NO | 6 | NO | YES | YES |
| 59Pr143 | 56 | NO | NO | NO | NO | NO |
| 60Nd143 | 4 | NO | 6 | NO | YES | YES |
| 60Nd144 | 38 | NO | 6 | NO | YES | YES |
| 60Nd145 | 14 | NO | 6 | NO | YES | YES |
| 60Nd146 | 57 | NO | 6 | NO | YES | YES |
| 60Nd147 | 62 | NO | 6 | NO | NO | NO |
| 60Nd148 | 40 | NO | 6 | NO | YES | YES |
| 60Nd150 | 60 | NO | 6 | NO | YES | YES |
| 61Pm147 | 11 | NO | NO | NO | NO | NO |
| 61Pm148 | 32 | NO | NO | NO | NO | NO |
| 61Pm148m | 21 | NO | NO | NO | NO | NO |
| 61Pm149 | 63 | NO | NO | NO | NO | NO |
| 61Pm151 | >68 | NO | 6 | NO | NO | NO |
| 62Sm144 | >68 | NO | 6 | NO | YES | NO |
| 62Sm147 | 27 | NO | 6 | NO | YES | YES |
| 62Sm148 | >68 | NO | 6 | NO | YES | NO |
| 62Sm149 | 7 | NO | 6 | NO | YES | YES |
| 62Sm150 | 16 | NO | 6 | NO | YES | YES |
| 62Sm151 | 10 | NO | 6 | NO | YES | NO |
| 62Sm152 | 8 | NO | 6 | NO | YES | YES |

**Table 1. Sources of capture gamma source data (Continued)**

| Isotope | Rank | JEFF-3.1 | ENDF/B-VII.0 | JENDL-3.3 | BNL Data | IAEA Data* |
|---|---|---|---|---|---|---|
| 62Sm153 | 66 | NO | 6 | NO | NO | NO |
| 62Sm154 | >68 | NO | 6 | NO | YES | YES |
| 63Eu153 | 9 | NO | 6 | 12 | YES | YES |
| 63Eu154 | 13 | NO | NO | NO | NO | NO |
| 63Eu155 | 12 | NO | NO | NO | NO | NO |
| 63Eu156 | 39 | NO | NO | NO | NO | NO |
| 63Eu157 | >68 | NO | 6 | NO | NO | NO |
| 64Gd155 | 53 | NO | 6 | NO | YES | YES |
| 64Gd156 | 35 | NO | 6 | NO | YES | NO |
| 64Gd157 | 26 | NO | 6 | NO | YES | YES |
| 64Gd158 | 51 | NO | 6 | NO | YES | NO |
| 65Tb159 | >68 | NO | NO | NO | YES | YES |
| 66Dy161 | >68 | NO | 6 | NO | YES | YES |
| 66Dy162 | >68 | NO | 6 | NO | YES | YES |
| 66Dy163 | >68 | NO | 6 | NO | YES | YES |

Note: 6/12 indicate the gamma source data are available either in MF6 or in MF12-15. Isotopes studied in CERES experiments also highlighted in blue. Note that these were aimed at burn-up credit in criticality and so are not always the highest ranking in reactor physics applications. In the second column, yellow indicates an isotope in the top 26 (90$^{th}$ percentile) for worth in a PWR.

*Data taken from the “nglist_a” (assessed) file.

Source: Jacobs Engineering Group Inc., 2020.

# 3. Nuclear data evaluations

In order to study the state of gamma source data within evaluated nuclear files, the types of data that are allowed must be briefly reviewed. This is followed by a discussion on the ways that these "raw" input data may be processed and then interpreted in simulation systems using industry-standard codes. This is followed by a review of the current state of evaluated nuclear data files from the major nuclear data evaluation projects.

## 3.1 Representation of gamma source data within ENDF-6 format evaluations

The ENDF-6 format (Cross-Section Evaluation Working Group 2018) defines different kinds of data within "file types" using the nomenclature "MF" and with values between 1 and 40. Within any MF, data are defined for different reaction identifiers using the nomenclature "MT" and various integer values associated with physically distinguishable reactions (e.g. fission, neutron capture, elastic scattering).

Traditionally, gamma radiation promptly emitted following neutron capture has been described in the "MF" sections 12 to 15. MF12 defines the multiplicity of gammas as a function of incident neutron energy. The multiplicity of all gammas is given first and then the multiplicity of each explicit gamma line is given. This is followed by the multiplicity of the continuum or remaining gamma spectrum when explicit line data are removed. At any defined incident energy, the sum of the line emissions and any continuum contribution should be equal to the total emission.

MF13 contains the gamma production cross-sections. Its use is generally not recommended since this quantity can be formed by coupling the cross-section in MF3 with the multiplicity in MF12. MF14 describes the angle of emission of gammas and if it is missing, their emission is assumed to be isotropic. MF15 contains the continuum distribution of any gammas not described by multiplicities. This integrates to unity so that it can be coupled with the continuum multiplicity at the end of MF12.

Application of nuclear data to higher incident neutron energies has introduced the need for many more reaction channels and even the necessity to combine channels (e.g. MT=5 or MT=10). These data are very important for fusion and other applications where neutrons with energy above a few MeV (i.e. 14 MeV deuterium-tritium neutrons) are present in significant numbers.

High-energy reactions can emit many different particles so it is appropriate to keep the energy distribution of these particles together. The angle and energy of the emitted particles are strongly correlated; hence, emission data are represented in the MF6 format, where full double-differential energy-angle data may be recorded. Above 20 MeV, the (n,γ) channel is extremely small and not of significant importance. Modern high-energy evaluations are typically very complete, so gamma emission from (n,γ) is represented in MF6 like all other data.

The structure of MF6 is complex relative to other file structures. However, the data often contain a fairly simple representation for (n,γ). The multiplicity of all gammas is given first as a function of incident neutron energy. Next, pairs of (gamma energy, intensity) are given for each discrete gamma line. Then, a continuum spectrum is given. There is no relative intensity of the spectrum to the lines.

## 3.2 Generation of heating and photon source data with the NJOY code

The nuclear data processing code (NJOY) (MacFarlane, 1994) makes use of gamma source data to generate heat production cross-sections, known as kinetic energy released per unit mass (KERMA), and to re-group photon source data into bins. If data are present in MF12, it forms the locally deposited heating (KERMA) as:

$$k_j(E) = \left(E + Q_j - \overline{E}_{j,n} - \overline{E}_{j,\gamma}\right)\sigma_j(E)$$

where:

$E$ is the incident neutron energy;

$j$ is the reaction channel;

$Q$ is the energy released by the reaction;

$\overline{E}_{j,n}$ is the mean energy attributed to emitted neutrons and hence not released locally;

$\overline{E}_{j,\gamma}$ is the mean energy attributed to emitted photons and hence not released locally;

$\sigma_j(E)$ is the reaction cross-section giving the probability of this local heating following neutron-nucleus interaction and reaction $j$ occurring; and

$\overline{E}_{j,\gamma}$ is formed from data in MF12 and MF15.

The distribution of the photon heating is then:

$$k_j^D(E) = \left(\overline{E}_{j,\gamma}\right)\sigma_j(E).$$

For MT=102 (n,γ) the KERMA reduces to:

$$k_j(E) = \left(E + Q_j - \overline{E}_{j,\gamma}\right)\sigma_j(E)$$

The code also includes a method of calculating the small energy given to the recoiling nucleus by gamma emission. There is an option in the HEATR module of NJOY to include the photon heating so that only the energy attributed to neutrons is subtracted (this is zero in the case of neutron capture or MT102). When this option is applied, the code calculates the heating using a substitution method:

$$k_j(E) = \left(E + Q_j\right)\sigma_j(E).$$

Thus, the photon spectra are not used. In the case where the MF6 representation is used in the data, the local heating is added as:

$$k_j(E) = \sum_l \overline{E}_{j,l}\sigma_j(E).$$

where $l$ indicates all emitted heavy or charged particles that will deposit energy locally (i.e. not neutrons or gammas). In the case of (n,γ), this is just the recoiling nucleus.

As above, there is an option in the HEATR module of NJOY to include the photon heating so that only the energy attributed to neutrons is subtracted (none in the case of MT102). When this option is applied, the code prints heating due to photons and to gamma recoil. Thus, the only time the photon data are needed is when the option to include photon energy is requested in HEATR and data are in the form of MF6. These data can be used to check that the energy generated with MF6 data corresponds to the Q value.

Where MF12 data are used, there is no need to check that these data yield the Q value given in MF3 with the neutron cross-sections.

## 3.3 Existing gamma source data within the evaluations

Prior to the initiation of the WPEC Subgroup 27, a survey was performed to determine which reactions and nuclides had gamma source data within the ENDF/B-VI.8, JEFF-3.0 and JENDL-3.3 nuclear data libraries.

Since the survey, the JEFF-3.1 evaluation (Koning et al., 2006) was released in May 2005 and ENDF/B-VII.0 (Chadwick et al., 2006) in December 2006. Table 1 defines which of the 89 leading fission products have gamma spectra for the (n,γ) reaction within these three evaluations.

As noted at the bottom of the table, the number 12 indicates representation by MF12-15 while the number 6 indicates that all the information is included within MF6. There is no mixing of data between the two representations for MT102 – (n,γ). In general, there may be mixing between reactions, some with MF6 and others with MF12, but not by energy range within any individual reaction.

The gamma source data in the latest ENDF/B-VII.0 evaluations contain either new theoretical data generated by the EMPIRE code (Herman et al., 2007) that is represented by MF6 or theoretical data generated by the Japanese CASTHY code (Igarasi and Fukahori, 1998) that is represented by MF12. In the latter case, the high-energy evaluation is taken from JENDL-3.3. The new JEFF-3.1 evaluations have MF6 data generated with TALYS (Koning et al., 2007).

## 3.4 Criteria for assessment of gamma source spectra

Within any study of the spatial heating distribution in matter, it is important to preserve the overall energy available. In terms of (n,γ) – $j$ the energy released is:

$$k_j(E) = (E + Q_j)\sigma_j(E).$$

The cross-section $\sigma_j(E)$ is defined in MF3 within the evaluation so when assessing gamma spectral data we need to make sure that:

$$M_\gamma\left(\sum_i E_\gamma^i I\left(E_\gamma^i\right)+\int_{s\in spectrum} E_s C(E_s)\right)=Q+E\ ,$$

where the quantities on the left hand side can also have dependence on incident neutron energy. $I\left(E_\gamma^i\right)$ indicates the intensity of explicit gamma rays of energy $E_\gamma^i$. $M_\gamma$ is the multiplicity (average number of) gamma rays emitted. When explicit gamma lines cannot be seen, the continuum spectrum of gamma-ray probabilities is given as: $E_s C(E_s)$. Here $E_s$ is again gamma energy that can overlap the energies $E_\gamma^i$, giving a background to the line intensity, as well as extending well beyond them. $C(E_s)$ is the relative probability of the continuum gamma rays at $E_s$.

It is important to note the general expression for gamma intensity at a distance $x$ from the source neutron interaction origin - $o$ is:

$$I_x = I_o \times e^{-\mu x} B(x)$$

The absorption coefficient $\mu$ is the sum of effects due to Compton scatter, photoelectric effects and pair production gamma interactions. The former two of these tend to decrease exponentially and dominate below ~2 MeV. This is illustrated in standard references, for example from (Bobin, 1959). This means that the higher energy gammas penetrate further within the reactor structure. This, in turn, means their intensity is important relative to the lower energy gammas. These statements are true in principle but vary considerably with build-up factors $B$ for different distances $x$.

# 4. Experimental data

There are many papers giving measurements of gamma rays induced by capture of thermal and resonance neutrons. Such measurements are cited in the Evaluated Nuclear Structure Data File (ENSDF) database[2] as part of the Nuclear Structure Analysis (Nichols and Tuli, 2007).

Many of the fission products are also present in natural elements. There are two major databases containing measured thermal capture gammas for isotopes of natural elements. Both include data from ENSDF. The first database was created, and is now maintained, by Brookhaven National Laboratory (BNL). There is no formal reference for this database but considerable efforts have gone into its development (Tuli, 1983).

In 2007, the International Atomic Energy Agency (IAEA) completed a Co-ordinated Research Project (CRP) resulting in a database and extensive documentation (Choi et al., 2007) on Prompt Gamma Activation Analysis (PGAA). The United States (US) evaluators participating in the assembly of the BNL database also participated in the CRP and contributed significant data. This database is not being further developed at present and represents a "snap shot" in time.

The EMPIRE and TALYS modelling codes obtain information from the Reference Input Parameter Library (RIPL) database (Belgya et al., 2006). In turn, RIPL relies upon information from ENSDF as indicated in (Nicholas and Tuli, 2007), so that model calculations are based on the same basic information.

## 4.1 Comparisons of the available data

The IAEA database includes absolute gamma intensities or other data from which the gamma intensities can be calculated. The BNL database gives the relative intensity to the most intense gamma line. For some nuclides the absolute intensity is available.

Both databases were downloaded, compared and analysed. As part of the process, the $I\left(E_\gamma^i\right)$ intensity of explicit gamma rays of energy $E_\gamma^i$ and multiplicity $M_\gamma$ were used to calculate the *Q* value as:

$$M_\gamma\left(\sum_i E_\gamma^i I'\left(E_\gamma^i\right)\right) = Q^{Calc}$$

2. Accessible at the following URL: www.nndc.bnl.gov/ensdf/.

In many cases with the BNL database, this calculation was not possible because absolute intensity was not available. Findings are shown in Table 2 for the IAEA database (which includes the *Q* value). A number of points emerged as follows, and similar points could be made for those BNL data that could be checked in this way.

- The multiplicity in some cases was less than one (this is clearly unphysical).
- A weighted sum of the gamma photon energies was significantly (10% or more) below the *Q* value in many cases.
- A weighted sum of the gamma photon energies was significantly (10% or more) above the *Q* value in some cases.
- For the two nuclides checked against the BNL data ($^{12}$C and $^{103}$Rh), it was clear there were significant differences.

The first three points above can be seen in Table 2. Correspondence with one of the contributors to the PGAA data (Rick Firestone of Lawrence Berkeley National Laboratories in the US) revealed that only the most intense photons were represented as individual gamma lines. For some nuclides, lines not represented can, however, account for a significant proportion of the energy. This explains why in some cases the weighted sum of the gamma lines was significantly less than the *Q* values, and why a multiplicity of less than one can be obtained (i.e. not all the gamma photons are being accounted for).

**Table 2. Checks on the IAEA PGAA data**

| Isotope | Abundance (%) | Derived multiplicity | Q(calc)/Q (%) |
|---|---|---|---|
| Kr83 | 11.5 | 2.81 | 41.43 |
| Y89 | 100 | 2.46 | 97.09 |
| Zr91 | 11.2 | 2.58 | 51.45 |
| Zr96 | 2.8 | 65.9 | 1 297.49 |
| Mo95 | 15.9 | 2.5 | 35.41 |
| Mo96 | 16.7 | 2.16 | 55.57 |
| Mo97 | 9.55 | 2 | 34.26 |
| Mo98 | 24.1 | 2.26 | 31.87 |
| Mo100 | 9.63 | 1.4 | 28.89 |
| Ru100 | 12.6 | 0.31 | 13.15 |
| Ru101 | 17.1 | 4.19 | 57.27 |
| Ru102 | 31.6 | 3.57 | 74.96 |
| Ru104 | 18.6 | 5.55 | 130.63 |
| Rh103 | 100 | 1.35 | 9.26 |
| Pd104 | 11.1 | 0.76 | 4.03 |
| Pd105 | 22.3 | 1.88 | 17.99 |
| Pd106 | 27.3 | 0.7 | 16.06 |
| Pd108 | 26.5 | 1.87 | 35.77 |
| Ag109 | 48.2 | 1.15 | 14.48 |

**Table 2. Checks on the IAEA PGAA data (Continued)**

| Isotope | Abundance (%) | Derived multiplicity | Q(calc)/Q (%) |
|---|---|---|---|
| Cd110 | 12.5 | 614 | 5 716.33 |
| Cd111 | 12.8 | 1.17 | 8.34 |
| Cd113 | 12.2 | 1.77 | 25.55 |
| In115 | 95.7 | 1.18 | 6.95 |
| I127 | 100 | 1.06 | 14.79 |
| Xe128 | 1.92 | 0.23 | 1.14 |
| Xe129 | 26.4 | 0.72 | 10.91 |
| Xe130 | 4.08 | 0.3 | 2.36 |
| Xe131 | 21.2 | 1.09 | 17.79 |
| Xe136 | 8.87 | 1.18 | 42.18 |
| Cs133 | 100 | 1.37 | 16.84 |
| Ba134 | 2.42 | 1.58 | 43.33 |
| La139 | 99.9 | 1.37 | 53.49 |
| Ce142 | 11.1 | 2.01 | 66.54 |
| Pr141 | 100 | 0.91 | 29.28 |
| Nd143 | 12.2 | 2.21 | 34.14 |
| Nd144 | 23.8 | 2.25 | 80.9 |
| Nd145 | 8.3 | 2.67 | 57.99 |
| Nd146 | 17.2 | 0.98 | 17.16 |
| Nd148 | 5.7 | 1.24 | 18.45 |
| Nd150 | 5.6 | 3.08 | 69.79 |
| Sm147 | 15 | 8.29 | 394.35 |
| Sm149 | 13.8 | 2.23 | 17.9 |
| Sm150 | 7.38 | 1.46 | 46.25 |
| Sm152 | 26.8 | 0.9 | 18.74 |
| Sm154 | 22.8 | 0.83 | 9.42 |
| Eu153 | 52.2 | 4.25 | 18.48 |
| Gd155 | 14.8 | 1.29 | 20.02 |
| Gd157 | 15.7 | 1.38 | 24.81 |
| Tb159 | 100 | 0.98 | 10.82 |
| Dy161 | 18.9 | 2.48 | 23.78 |
| Dy162 | 25.5 | 2.02 | 30.14 |
| Dy163 | 24.9 | 1.2 | 11.01 |

Source: Jacobs Engineering Group, Inc. (2020).

## 4.2 Fission products with missing data sources

23 of the 89 fission products of interest are not represented in the IAEA or BNL gamma source databases. Of particular concern are those isotopes present in the top 26, including $^{93}$Zr, $^{107}$Pd, $^{135}$Xe, $^{147,148m}$Pm and $^{154,155}$Eu. Table 3 shows their predicted relative reactivity worth for PWR fuel irradiated to 60 GWd/te over 4 years.

None of the three evaluations considered contain gamma source data within their evaluations for these nuclides. The final column of Table 3 indicates that there are data in the TALYS-based Evaluated Nuclear Data Library (TENDL-2008) (Koning and Rochman, 2008) for some of these nuclides.

An enquiry to scientists at Conseil européen pour la recherche nucléaire (CERN) noted that measurements of prompt gammas from $^{135}$Xe could not be realistically performed for at least 10 years despite their ability to measure shorter-lived nuclides. It thus appears to be the case that the only way to obtain a gamma spectrum for important short-lived isotopes at present is to rely upon model calculation codes such as TALYS, EMPIRE, CASTHY or another gamma cascade modelling code.

**Table 3. Important fission products with no data in PGAA or BNL Databases**

| Isotope | Half-life | Rank | Worth | TENDL2008 |
|---|---|---|---|---|
| 54-Xe-135 | 9.14h | 1 | 10.842 | Y |
| 61-Pm-147 | 2.6234y | 11 | 3.370 | Y |
| 63-Eu-155 | 4.753y | 12 | 3.278 | N |
| 63-Eu-154 | 8.590y | 13 | 2.940 | N |
| 61-Pm-148m | 41.23d | 21 | 1.145 | N |
| 46-Pd-107 | 6.5E6y | 23 | 0.838 | N |
| 40-Zr-93 | 1.53E6y | 24 | 0.727 | Y |

Source: Jacobs Engineering Group, Inc. (2020).

## 4.3 Difficulties in measuring complete gamma spectra

Neutron cross-section curves show resonances that correspond to quantum states in the compound nucleus. Figure 1 shows the total cross-section for $^{19}$F, $^{95}$Mo and $^{235}$U from JEFF-3.1. For the light nuclide $^{19}$F, resonances start at around 27 keV. For the fission product $^{95}$Mo, the resonances start at around 45 eV and for the actinide $^{235}$U they begin at 0.3 eV. Resonance spacing is wave dependent but again tends to vary with mass. The position of the resonance is identified by Time of Flight (TOF) measurements. Capture measurements need not identify the full gamma cascade but they must determine that there are emitted gammas at this incident neutron energy.

**Figure 1. Total cross-sections for $^{19}$F, $^{95}$Mo and $^{235}$U**

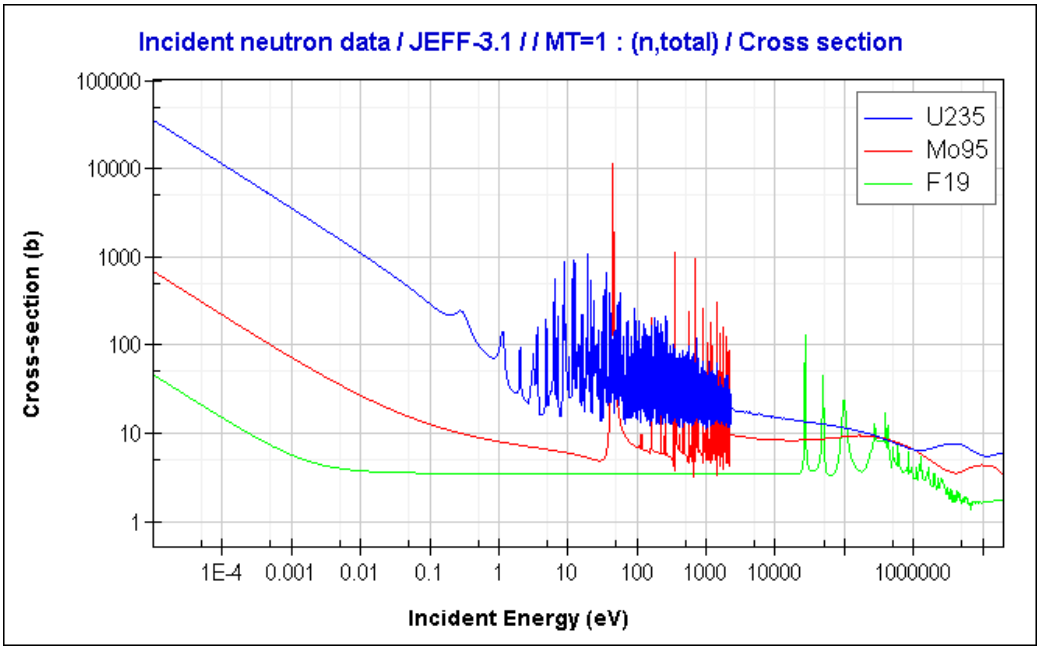


Source: NEA, 2020.

The best detectors, for example the 161 $BaF_2$ detectors in the Detector for Advanced Neutron Capture Experiments (DANCE) facility at Los Alamos (Sheets, 2007), collect gammas in bins whose width is on the order of 1 keV.

For a single resonance, the energy of the level produced is the neutron separation energy (several MeV) plus the energy of the resonance. As noted above, this is on the order of keVs for the light nuclei but of order eV for larger mass nuclei. The neutron separation energy is accurate to some tens of eV according to (Audi et al., 2003) although many Q values in the evaluations are rounded with less accuracy. It is important to recognise that the convention in Audi et al. is to tabulate the separation energy with the compound nucleus, whereas the *Atlas of Neutron Resonances* (Mughabghab, 2006) tabulates it against the target nucleus.

Hence, the detectors can identify the levels initiating cascade for light nuclides. This is not possible for heavy nuclides. Sheet notes: "The complete level scheme and their decay modes include both the quasi-continuum and discrete regions" (Sheet et al., 2007) when considering $^{95}$Mo. They use the cascade code DICEBOX (Bečvář, 1998) to model the continuum and discrete gammas.

# 5. Investigations

The method of production of a compound nucleus leads to different populations of initial quantum states and hence different decay schemes. The gamma cascade following beta decay to a nucleus will be different from the cascade for the same nucleus formed from neutron capture. Results from many particle-induced reactions help define the levels and gamma rays defined in the EXFOR database (Otsuka et al., 2014). The RIPL database contains the explicit levels generated from EXFOR, which includes all modes of nuclei production and not just those from neutron capture.

Since the lower energy levels are often formed from cascade, model codes such TALYS (and therefore the data within the TENDL-2008 library) contain explicit gammas from decay of the lower levels plus a continuum believed to be formed by binning gammas emitted from the higher states following a cascade model.

The TALYS code has also been used to generate data for evaluations in JEFF-3.1. The Q value check was considered on one of these files, $^{40}$Ca. First, corrections had to be applied to NJOY to achieve sensible results. Even when these corrections were applied, the results for $^{40}$Ca in the JEFF file were found to be seriously inconsistent with the Q value for (n,γ). Data for $^{135}$Xe were then taken from the TENDL-2008 library and processed. Again, the energy release was lower than expected by approximately 3 MeV per capture.

Detailed analyses were performed and results were found to be consistent with the outputs from the NJOY code, showing there were problems with the evaluation. In order to investigate the shortfalls, additional analyses were carried out with the evaluated data for $^{19}$F, the lightest nuclide in the TENDL-2008 library.

## 5.1 Fluorine investigation

The ENDF/B-VI.8 (McLane et al., 2001) file for $^{19}$F includes explicit gamma lines from Frankle's work (Frankle et al., 2001). At thermal incident neutron energies there are no continuum data. All information for the $i$ gamma rays is provided in MF=12. The intensities sum to the total number of gammas emitted, e.g.:

$$I_\gamma = \sum_i I\left(E_\gamma^i\right).$$

The energy release is also correctly formulated so that:

$$\sum_i E_\gamma^i I\left(E_\gamma^i\right) = Q.$$

The TENDL-2008 file for $^{19}$F includes discrete gamma lines for the low-energy gammas with continuum data for the higher energy cascade. The energy release within the TENDL file was incorrect. However, the intensities for the low-energy gammas were close to those in the ENDF/B-VI.8 without any multiplicity factors.

From these data, to find the total number of gammas one must take:

$$M_\gamma = \left( \sum_i I\left(E_\gamma^i\right) + \int_{s \in spectrum} C\left(E_s\right) \right).$$

But in the MF6 format, $M_\gamma$ is given as a multiplier, hence:

$$\left( \sum_i I'\left(E_\gamma^i\right) + \int_{s \in spectrum} C'\left(E_s\right) \right) = 1.$$

This is true in the file, but one would then expect that:

$$I'\left(E_\gamma^i\right) = \frac{I\left(E_\gamma^i\right)}{M_\gamma},$$

while instead the relation that is found in the data is:

$$I'\left(E_\gamma^i\right) \approx I\left(E_\gamma^i\right).$$

The next point to question is how the multiplicity was set. In order to preserve energy release, one should apply the equation:

$$\sum_i E_\gamma^i I\left(E_\gamma^i\right) = Q,$$

where $i$ includes all possible gammas. As some gammas are included in the continuum this changes to: $\sum_i E_\gamma^i I\left(E_\gamma^i\right) + \int_{s \in spectrum} E_s C\left(E_s\right) = Q$,

or: $M_\gamma \left( \sum_i E_\gamma^i I'\left(E_\gamma^i\right) + \int_{s \in spectrum} E_s C'\left(E_s\right) \right) = Q.$

A detailed review of the BNL database of thermal capture gammas indicates little change since the original work by Frankle. Further, the absolute intensity of the strongest gamma ray is given. This enabled all the gammas to be included in an ENDF-6 structured file and consistency with the *Q* value to be achieved. This again means that the intensities of the discrete gammas in the TENDL file seem to require a reduction by the multiplicity.

### *5.1.1 Suggested procedure for improving energy balance of (n,γ) in TENDL*

The issues identified above with the TENDL data could be addressed with a simple procedure to ensure energy balance in neutron capture. Current discrete intensities should be reduced by the multiplicity:

$$I'\left(E_\gamma^i\right) = \frac{I\left(E_\gamma^i\right)}{M_\gamma},$$

where $I'\left(E_\gamma^i\right)$indicates the new intensity, $I\left(E_\gamma^i\right)$ indicates the existing intensity at energy $E_\gamma^i$ and $M_\gamma$ is the existing multiplicity. All terms have implicit dependence on the incident neutron energy.

Next, the energy release from the discrete lines should be formed by separating the *Q* value into two components for the continuum and discrete lines, such that:

$$M_\gamma \sum_i E_\gamma^i I'\left(E_\gamma^i\right) = Q(lines) \text{ and}$$

$$M_\gamma \int_{s \in spectrum} E_s C'(E_s) dE_s = Q(continuum), \text{ where}$$

$$Q(continuum) = Q - Q(lines).$$

In this way, the remaining energy from the continuum spectrum is formed and the spectral intensities should be scaled to satisfy the condition that:

$$C'(E_s) = C(E_s) \frac{Q(continuum)}{M_\gamma \int_{s \in spectrum} E_s C(E_s) dE_s}.$$

Now we have consistency with the Q value but the ENDF format requires a normalisation constraint:

$$\sum_i I''\left(E_\gamma^i\right) + \int_{s \in spectrum} C''(E_s) = 1.$$

As a result:

$$M_\gamma'' \left( \sum_i E_\gamma^i I''\left(E_\gamma^i\right) + \int_{s \in spectrum} E_s C''(E_s) \right) = Q, \text{ where:}$$

$$M_\gamma'' = M_\gamma \left( \sum_i I'\left(E_\gamma^i\right) + \int_{s \in spectrum} C'(E_s) \right),$$

$$I_\gamma'' = \frac{I_\gamma'}{\left( \sum_i I'\left(E_\gamma^i\right) + \int_{s \in spectrum} C'(E_s) \right)}, \text{ and}$$

$$C_\gamma'' = \frac{C_\gamma'}{\left( \sum_i I'\left(E_\gamma^i\right) + \int_{s \in spectrum} C'(E_s) \right)}.$$

These changes were applied in a separate analysis and then they were placed in an updated version of the TENDL file. This was processed with the NJOY code to compute heating with the HEATR module and photon emission at 10 μeV using the GROUPR module. The *Q* value was correctly reproduced, as was the gamma emission cross-section.

Figure 2 shows the resulting spectra. The TENDL-2008 continuum spectra are discretised into 41 histogram bins and this structure was preserved in the study to prevent any re-grouping effects. The solid green line shows the measured data from the ENDF/B-VI.8 evaluation and the dotted blue line was generated from the TENDL-2008 evaluation.

TENDL-2008 contains explicit gammas from the lower few quantum levels and the intensity (probability) of these can be seen to be above the solid line. When the scaling has been applied, these are usually, but not always, below the solid line.

The measured spectra are somewhat above the TENDL-2008 dotted blue line for more penetrative gammas above 2 MeV. After scaling, the red dashed line initially becomes higher then drops down above 5 MeV. Review of the $^{19}$F data indicates the TENDL-2008 spectrum is not a good fit to the known gamma lines. However, without further information this approximate shape from RIPL will continue to be used.

**Figure 2. Gamma-ray emission spectra for $^{19}$F**

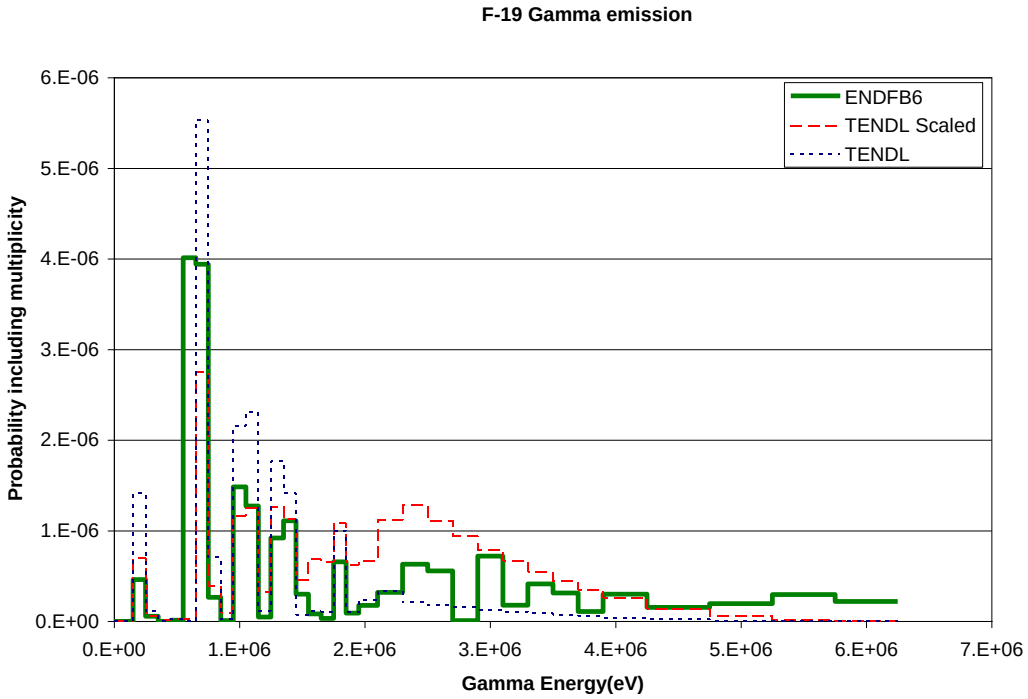


Source: Jacobs Engineering Group, Inc. (2020).

## 5.2 Application to $^{95}$Mo

The ENDF/B-VII.0 library includes a new evaluation for $^{95}$Mo. The evaluation resulted from the work of the WPEC Subgroup 23 (NEA, 2009). It includes gamma source data generated by the EMPIRE code (Herman et al., 2007), using the RIPL database (Belgya et al., 2006), which is the same database used in TENDL-2008.

Measurements of gamma emission spectra from $^{95}$Mo have taken place at the DANCE facility (Sheets, 2007). Calculated and measured two-step cascade gamma-ray energy spectra for particular resonances are given in 150 keV energy bins. The multiplicity spectra giving the probability of one to eight co-incident gammas are also given. Another paper (Sheets, 2006) shows extension to the work to cover spectra for two, three, four co-incident gammas. It is clear that if up to eight co-incident gammas can be measured and weighted with the multiplicity spectrum, then the overall gamma spectrum could be formed.

Calculations with the NJOY code using the ENDF/B-VII.0 $^{95}$Mo file showed a slight mismatch in energy release. The results from NJOY yielded 9.395 MeV per capture at thermal incident neutron energies whereas the *Q* value is 9.154 MeV. The gamma spectra in the ENDF/B-VII.0 evaluation are fairly smooth until one gets to emission energies close to the neutron separation energy, where there is significant structure. Figure 3 shows the spectra at thermal energies. There is expected structure at low gamma energies, where the gamma line intensity tends to be known, but also at gamma energies close to the neutron separation energy. The graph is logarithmic to show this structure in low-intensity gammas.

**Figure 3. Gamma-ray emission spectrum for $^{95}$Mo**

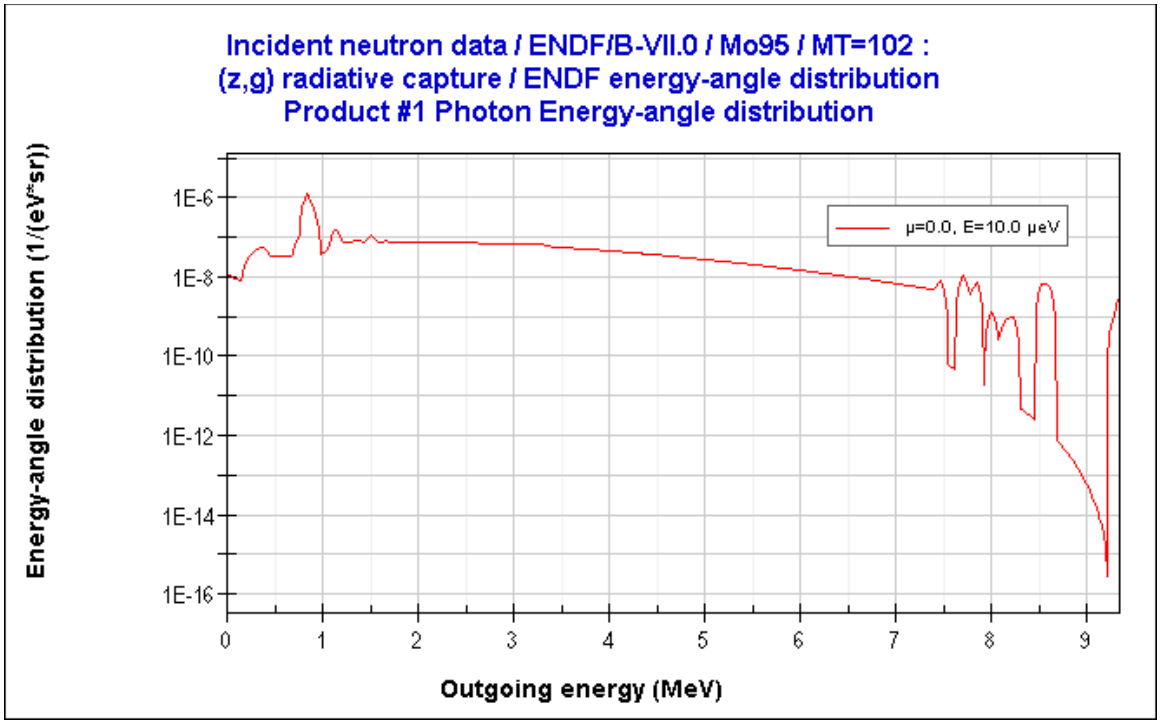


Source: NEA, 2020.

Further review of the spectra shows that the shape of this high-energy structure does not change as incident neutron energy increases up to 200 keV. Above this, there is a systematic shift as shown in the zoomed Figure 4.

**Figure 4. High-energy spectra tails for $^{95}$Mo**

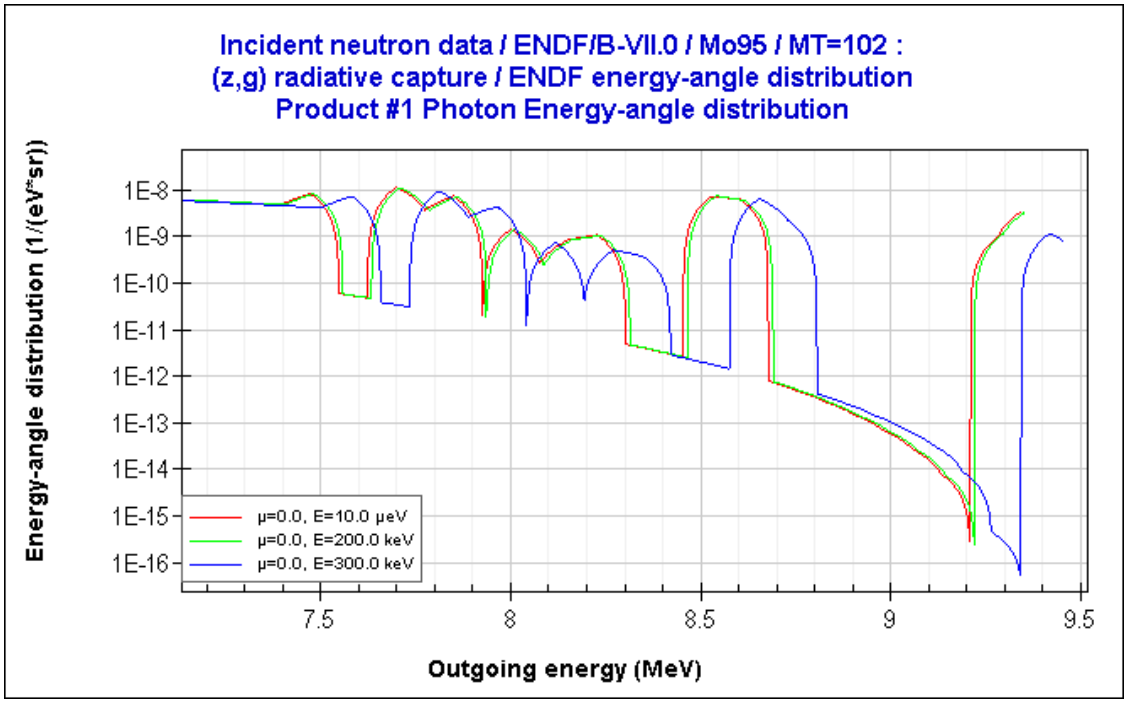


Source: NEA, 2020.

Investigations into the nature of the evaluations found that the high-energy end of the photon spectrum is composed of transitions from the compound nucleus state directly to discrete low-energy states (i.e. the ground state, 1$^{st}$ excited state) of the final nucleus. This information explains the high-end structure. The majority of photons in decaying cascades (about three photons per cascade on average) are of smooth statistical nature with a possible discrete transition in the last step of the cascade. Hence, one can again see some structure at low photon energies. Discrete transitions are in principle delta functions and these were appropriately broadened to make evaluated spectra look closer to the experimentally observed spectra. This is done also for the discrete transition to the ground state, resulting in small energy excess above *Q* value.

In Figure 3, the highest energy peak is well above the neutron binding energy of 9.154 MeV. The other high-energy structure does not seem to correspond to neutron binding energy minus the energy of each of the lowest levels. These tend to decay with single gammas and exist for measurable times from 0.06 ns to 0.7 ps, although there are the correct number of levels to correspond with high-energy peaks. This is assuming that data were taken from RIPL and that the level at 1.33 MeV, questioned in the latest 2008 ENSDF file, does not exist. It was also noted that the methodology in EMPIRE was checked fairly carefully on the sample cases of Fe and Ge (Iwamoto et al., 2004). Review of this paper indicated that whereas the overall high-energy gamma cascade in reactions at high neutron energy was validated, there was no direct validation of (n,γ). At the high energies concerned, reactions other than (n,γ) dominate.

From this review, the high-energy structure in the ENDF/B-VII.0 evaluation requires further justification. The overall gamma cascade following neutron capture is modelled in both EMPIRE and TALYS. In addition, there is a JEFF-3.1 evaluation that is taken from

an early ENDF/B-VII.0 evaluation, later replaced when the EMPIRE generated evaluation was adopted. The JEFF-3.1 evaluation can thus be assumed to have been superseded.

**Figure 5. TENDL and EMPIRE-based gamma spectra for $^{95}$Mo**

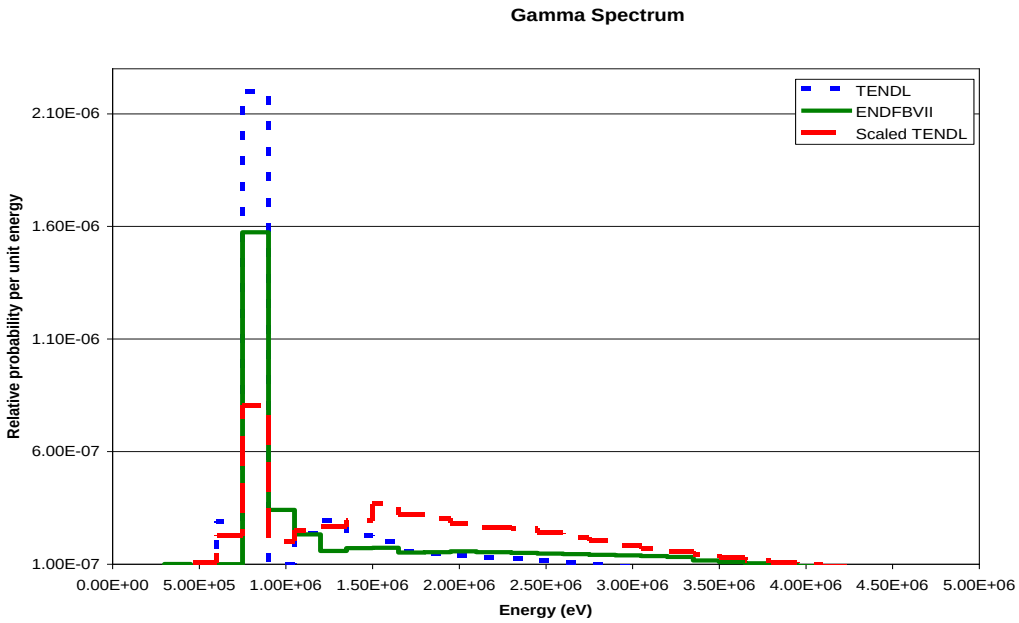


Source: Jacobs Engineering Group, Inc. (2020).

Sheets et al. (2007) published incomplete gamma-ray spectra measured in a significant S-wave resonance at 554 eV. EMPIRE and TENDL spectra for neutron energies in the range 550 to 560 eV were collected in the 22 gamma bins applied in the WIMS code using the NJOY code. Figure 5 shows the spectra on a linear y-axis. The TENDL data again did not preserve the energy generated and the dotted blue line is adjusted as described above to produce the dashed red line. This peaks in the same 750 keV to 1 MeV bin as the EMPIRE-based ENDF/B-VII.0 evaluation, but the upper energy continuum contribution is larger.

**Figure 6. TENDL and EMPIRE-based gamma spectra for $^{95}$Mo (log scale)**

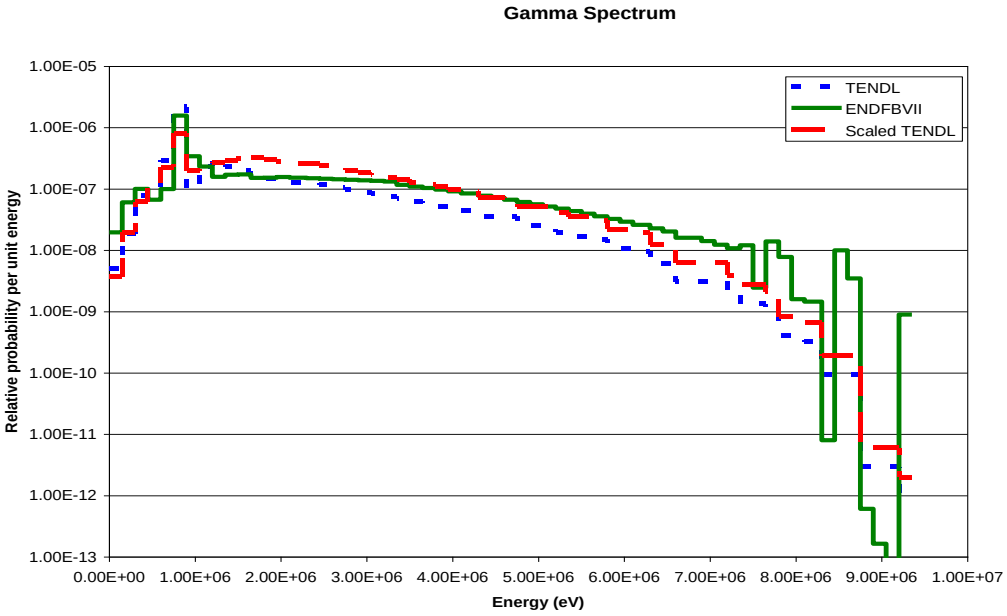


Source: Jacobs Engineering Group, Inc. (2020).

The same curve is reproduced on a log scale in Figure 6 and shows the high-energy delta functions in the EMPIRE (ENDF/B-VII.0) file that are missing from TENDL. The JENDL-3.3 evaluation also contains gamma emission data for $^{95}$Mo. These were checked and found to preserve the *Q* value. They are shown in Figure 7.

**Figure 7. Gamma spectra for $^{95}$Mo from JENDL-3.3, ENDF/B-VII.0 and TENDL-2008**

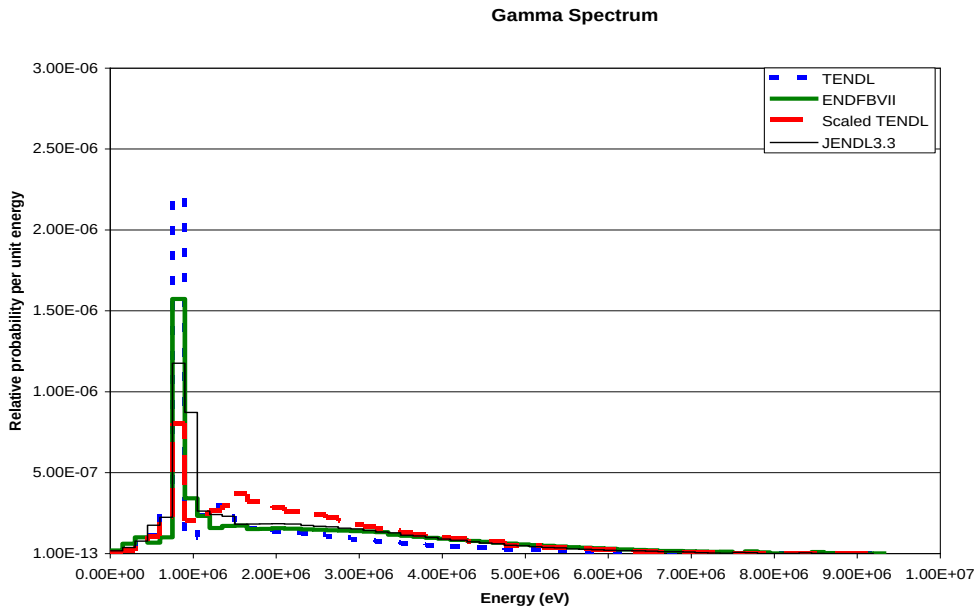


Source: NEA, 2020.

For emission energies above 1.5 MeV, the CASTHY spectra from JENDL-3.3 appear very similar to the EMPIRE spectra from ENDF/B-VII. Below this, where one would expect the gammas to be better known they are dissimilar. Figure 8 shows the high-energy tail of the CASTHY spectrum. This also shows considerable structure but at different gamma energies from the EMPIRE spectra.

**Figure 8. Gamma spectra for $^{95}$Mo from JENDL-3.3, ENDF/B-VII.0 and TENDL-2008 (log scale)**

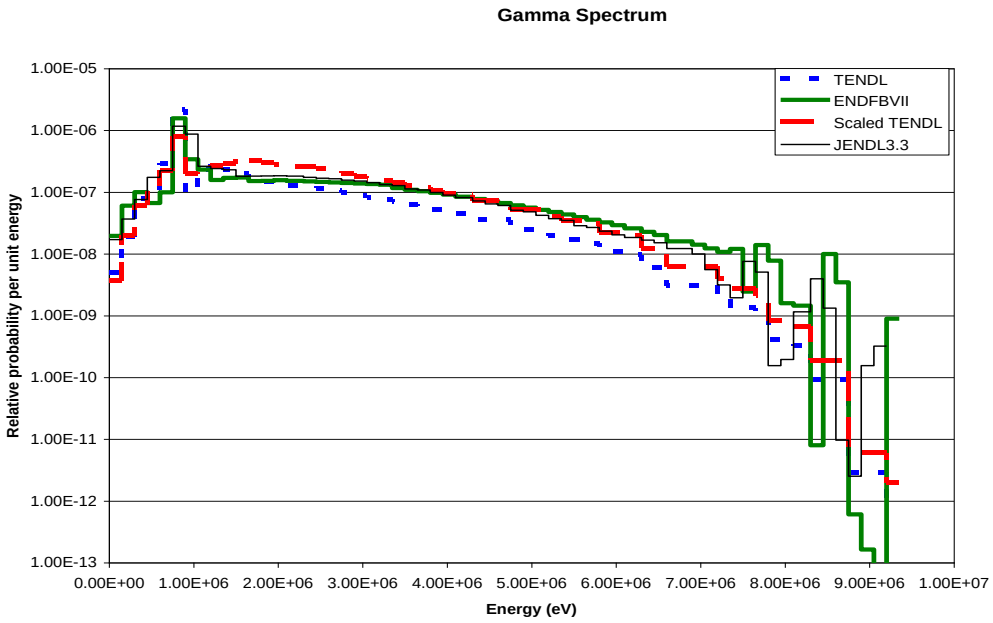


Source: Jacobs Engineering Group, Inc. (2020).

## 5.3 High-energy structure in gamma spectra

The gamma spectra from thermal neutron capture in other high-priority fission products were reviewed graphically using a development version of the Java-Based Nuclear Data Information System (JANIS) (Soppera, 2014), developed by the NEA.

The Zr and Pd isotopes, with one exception, contain small high-energy structures, whereas $^{95}$Mo and $^{127}$I do not. The previous structure seen for Mo was introduced at higher incident neutron energies. The $^{91}$Zr data includes a significant peak between 6.3 and 6.5 MeV (with a Q value of 8.635 MeV), as shown in Figure 9.

**Figure 9. High-energy gamma spectrum tail for $^{91}$Zr**

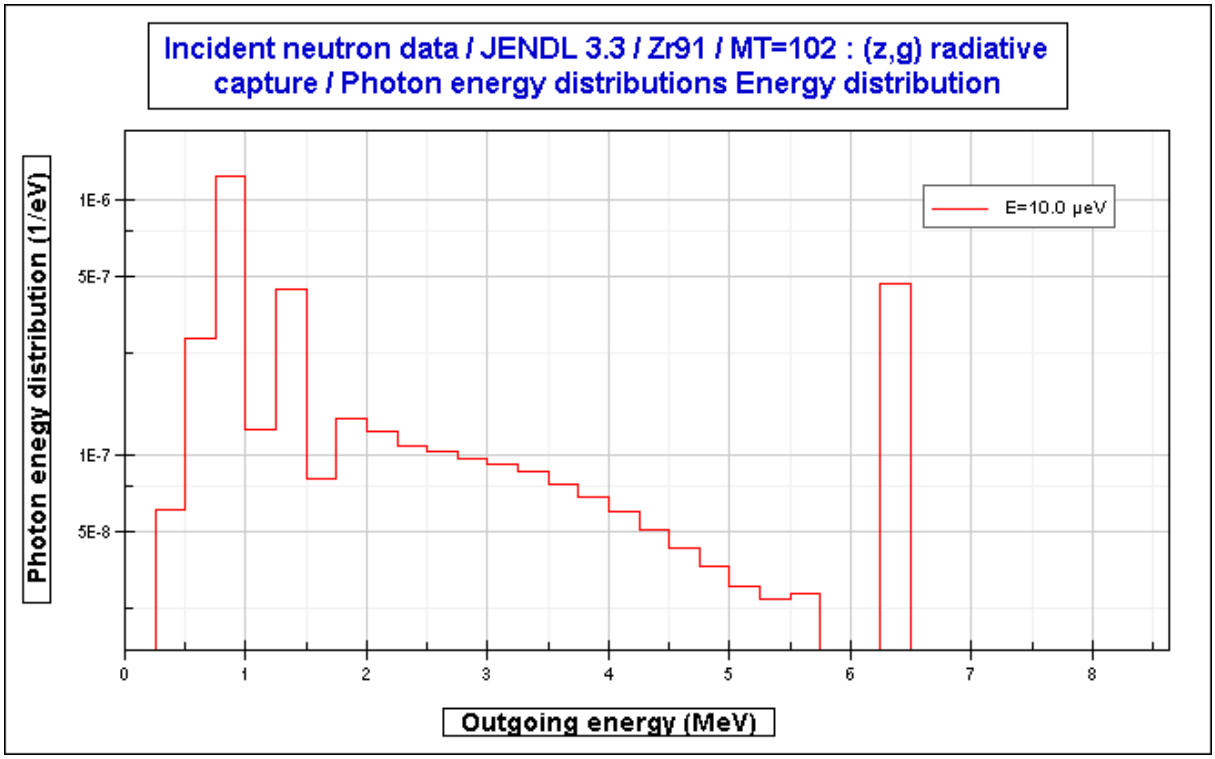


Source: NEA, 2020.

Examining EXFOR for $^{92}$Zr levels, one finds some high-energy levels and description of an M1 giant resonance. These are seen from particle-induced reactions but not for neutron capture. This is suspected to have been introduced by automatic processing of data into RIPL.

# 6. Photon production for other materials

In parallel with the work on fission product photon production, new gamma production evaluations were developed for other nuclei of interest in nuclear energy applications. Advanced light water reactors (LWR) and new experimental facilities such as the Jules Horowitz Reactor (JHR) require accurate information on the local energy deposition, which depends on precise modelling of photon energy deposition. This, in turn, requires data on the photon production from nuclear reactions on the constituent materials of the reactor, including elements such as iron and nickel within steels and silver, indium, cadmium and gadolinium, which are found in control rods and/or burnable poisons. A rigorous study of the photon production for the naturally occurring isotopes of those elements found inconsistencies and errors that motivated re-evaluations (Ravaux et al., 2013).

**Figure 10. Ratio of the database integral discrete gamma energy ($Q_\gamma$) to the total gamma emission energy ($B_n$)**

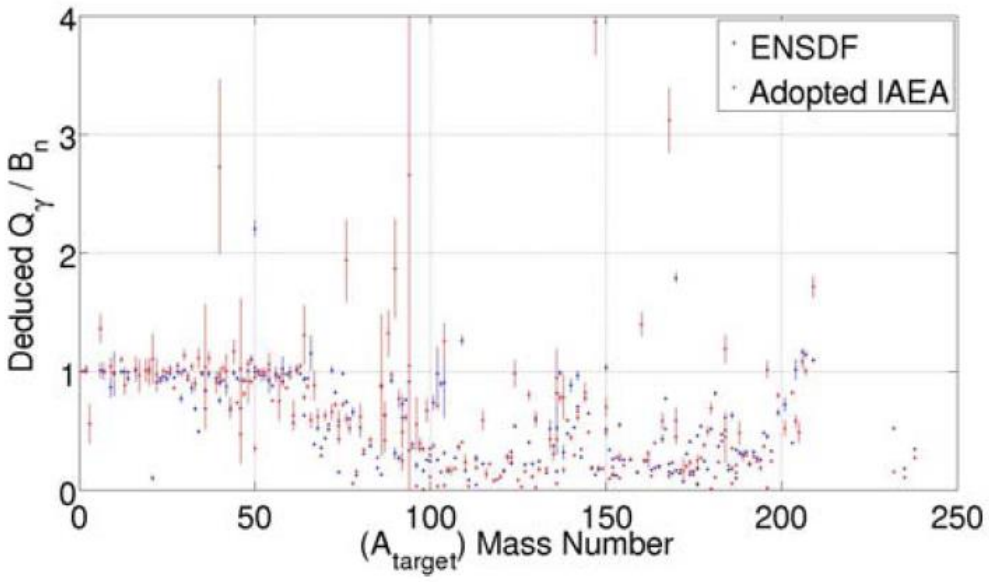


Source: Ravaux et al., 2013.

The IAEA has co-ordinated the production and maintenance of the Evaluated Gamma-ray Activation File (EGAF) (IAEA, 2007), which is a database of more than 30 000 prompt gamma rays and more than 3 000 radioactive decay gamma rays, covering isotopes ranging from hydrogen to uranium. This includes gamma production spectra based on evaluations using the ENSDF database, complemented with other thermal neutron measurements. A comprehensive comparison of the total integrated photon energy from the IAEA database and ENSDF against the correct energy emission value is depicted in Figure 10. For heavier isotopes, particularly above a baryon number of 70, neither of the databases contain the

complete energy and the continuum contribution must be included in some process. To address this issue, the TALYS nuclear reaction code was used to simulate gamma cascades after neutron capture. The built-in Generalised Lorentzian strength function and Gilbert-Cameron composite level density model were used in Hauser-Feshbach decay simulations using discrete levels within the RIPL database. These spectra are a complement to the lower energy discrete data taken from the established EGAF database. Results for four isotopes are shown in Figure 11, compared against the JEFF-3.1.1 library data.

**Figure 11. Gamma production spectra for thermal neutron capture in a set of important isotopes for nuclear energy applications**

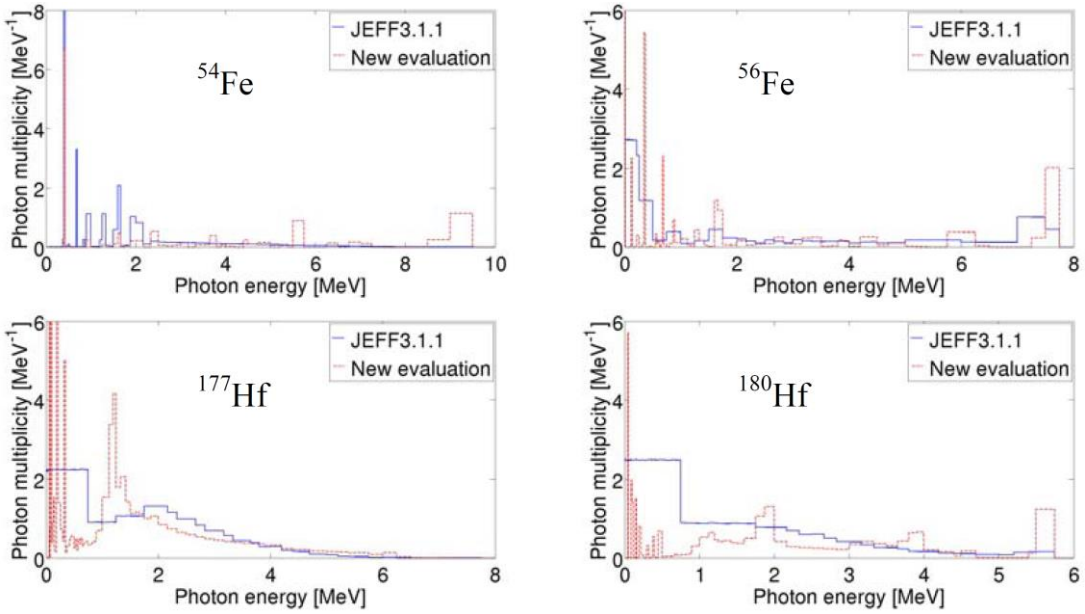


Source: Ravaux et al., 2013.

The evaluated gamma spectra were processed within complete nuclear data files and tested in simulations using the TRIPOLI-4.7 Monte Carlo radiation transport code. In some cases, such as $^{54}$Fe, the integral energy has been corrected and total heating increases in general. For the important case of $^{56}$Fe, the spectrum is shifted to higher energies that are more penetrative and change the local heating within components such as stainless steel reflectors. To demonstrate this feature, the PERLE experiments (Vaglio-Gaudard et al., 2010) conducted at the EOLE zero-power reactor were simulated, with JEFF-3.1.1 local deposited gamma dose lower by up to 2.3% when compared with the updated $^{56}$Fe gamma spectra. More information and details can be found in (Ravaux, 2014).

# 7. Conclusions

Currently, it is not possible to measure complete gamma spectra for fission products. Theoretical prompt gamma spectra from one of the three model codes (CASTHY, EMPIRE, TALYS) should be added to evaluated files for fission products. As these are the most important for thermal reactors, only data for the (n,γ) channel should be added.

Whereas the BNL and IAEA databases for Prompt Gamma Activation Analysis (PGAA) serve a valuable purpose in identifying material present in consignments, they are not a suitable source for spectral data in the evaluated files as the energy balance is not preserved. The energy formed by coupling the gammas with their intensity is sometimes larger than the energy available by considerable amounts. This may be a question of quality assurance or it may be due to inaccurate thermal capture cross-sections or indeed absolute gamma intensities (which are often missing from the BNL version of the database). One would expect the energy produced to be short of the Q value as not all gamma lines are accounted for. It often is, but there is no obvious trend with mass.

It is recommended that corrections be made to the gamma spectra from TALYS to preserve energy balance, which is currently short by several MeV. These should be reviewed by the code authors, applied or adapted as they think fit. The structure seen in CASTHY and EMPIRE gamma spectra (and hence present in ENDF/B-VII.0) is questionable. These need to be investigated before such spectra are included in the files.

Data with corrections to preserve energy balance should be included for the 89 important fission products identified in Table 1 and new files should be created for those that were not yet available at the time of this work.

The impact of improved gamma spectra for other materials within nuclear reactors on local gamma heating and dose rates is non-negligible and this area of study deserves more attention to reduce uncertainties and allow for longer-term operation of facilities.

# *References*


Audi, G., A.H. Wapstra and C. Thibault (2003), "The AME2003 atomic mass evaluation: (II). Tables graphs and references", *Nuclear Physics A*, 729, pp. 337-679, DOI: 10.1016/j.nuclphysa.2003.11.003.

Bečvář, F. (1998), "Simulation of γ cascades in complex nuclei with emphasis on assessment of uncertainties of cascade-related quantities", *Nuclear Instruments and Methods in Physics Research A*, 417, 2-3, pp. 434-449, DOI:10.1016/S0168-9002(98)00787-6.

Belgya, T., O. Bersillon, R. Capote Noy, T. Fukahori, G. Zhigang, S. Goriely, M. Herman, A.V. Ignatyuk, S. Kalias, A.J. Koning, P. Oblozinsky, V.Plujko and P.G. Young (2006), *Handbook for Calculations of Nuclear Reaction Data*, IAEA-TECHDOC-1506, International Atomic Energy Agency, Vienna.

Bobin, K.J. (1959), *A Nuclear Physics Training Manual*, AERE-N/M 11D, UK Atomic Energy Research Establishment.

Chadwick, M.B. et al. (2006), "ENDF/B-VII.0: Next generation evaluated nuclear data library for nuclear science and technology", *Nuclear Data Sheets* 107, 12, pp.2931-3060, DOI: 10.1016/j.nds.2006.11.001.

Choi, H.D., R.B. Firestone, R.M. Lindstrom, G.L. Molnár, S.F. Mughabghab, R. Paviotti-Corcuera, Z. Révay, A. Trkov, V. Zerkin and C.M. Zhou (2007), *Database of Prompt Gamma Rays from Slow Neutron Capture for Elemental Analysis*, STI/PUB/1263, International Atomic Energy Agency, Vienna.

Cross Section Evaluation Working Group (2018), *ENDF-6 Formats Manual: Data Formats for the Evaluated Nuclear Data Files ENDF/B-VI, ENDF/B-VII and ENDF/B-VIII*, BNL-203218-2018-INRE, ENDF-102, Brookhaven National Laboratory, Upton, New York.

Frankle, S.C., R.C. Reedy and P.G. Young (2001), *Improved Photon-Production Data for Thermal Neutron Capture in the ENDF/B-VI Evaluations*, LA-13812, Los Alamos National Laboratory, Los Alamos.

Herman, M., R. Capote, B.V. Carlson, P. Obložinský, M. Sin, A. Trkov, H.Wienke and V. Zerkin (2007), "EMPIRE: Nuclear reaction model code system for data evaluation", *Nuclear Data Sheets*, Volume 108, Issue 12, pp. 2655-2715, DOI: 10.1016/j.nds.2007.11.003.

IAEA (2007), *Database of Prompt Gamma Rays from Slow Neutron Capture for Elemental Analysis*, ISBN 920101306X, International Atomic Energy Agency, Vienna.

Igarasi, S. and T. Fukahori (1998), *Program CASTHY Statistical Model Calculation for Neutron Cross Sections and Gamma Ray Spectrum*, JAERI-1321, NEANDC(J)-156/U, INDC(JPN)-143/L.

Iwamoto, O., M. Herman, S.F; Mughabghab, P. Obložinský and A. Trkov (2005), "Neutron cross-section evaluations for $^{70,72,73,74,76}$Ge", *International Conference on Nuclear Data for Science and Technology 2004, AIP Conference Proceedings* 769, 434, DOI:10.1063/1.1945041.

Koning, A.J., R. Forrest, M. Kellett, R. Mills, H. Henriksson and Y. Rugama (2006), *The JEFF-3.1 Nuclear Data Library*, NEA No. 6190, ISBN 92-64-02314-3, JEFF Report 21, OECD Publishing, Paris, www.oecd-nea.org/jcms/pl_36784/the-jeff-3-1-nuclear-data-library.

Koning, A.J., S. Hilaire and M. Duijvestijn (2007), "TALYS-1.0", *Proceedings of the International Conference on Nuclear Data for Science and Technology 2007*, 1, pp. 227, DOI:10.1051/ndata:07767.

Koning, A.J. and D. Rochman (2012), "Modern nuclear data evaluation with the TALYS code system", *Nuclear Data Sheets* 113, 12, pp. 2841-2934, DOI:10.1016/j.nds.2012.11.002.

Koning, A.J., D. Rochman, J.–Ch. Sublet, N. Dzysiuk, M. Fleming, S; van der Marck (2019), "TENDL: Complete nuclear data library for innovative nuclear science and technology", *Nuclear Data Sheets* 155, 1, pp. 1-55, DOI:10.1016/j.nds.2019.01.002.

MacFarlane, R. E and D. G. Muir (1994), *The NJOY Nuclear Data Processing System Version 91*, LA-12740-m, UC-415, Los Alamos National Laboratory, United States.

McLane, V. et al. (1996), *ENDF/B-VI Summary Documentation*, BNL-NCS-17541 4th Edition, ENDF-201, Brookhaven National Laboratory, Upton, New York.

Mughabghab, S. (2018), *Atlas of Neutron Resonances*, 6th Edition, ISBN 9780444637796, Elsevier Science.

NEA (2005), *Assessment of Neutron Cross-section Evaluations for the Bulk of Fission Products*, International Evaluation Co-operation, Volume 21, NEA/WPEC-21 Report, OECD Publishing, Paris, www.oecd-nea.org/jcms/pl_13958.

NEA (2009), *Evaluated Data Library for the Bulk of the Fission Products*, International Evaluation Co-operation, Volume 23, NEA/WPEC-23 Report, OECD Publishing, Paris, www.oecd-nea.org/jcms/pl_14316.

Newton, T., G. Hosking, L. Hutton, D. Powney, B. Turland and T. Shuttleworth (2008), "Developments within WIMS10", *Proceedings of the International Conference on the Physics of Reactors and Nuclear Power: A Sustainable Resource*, Interlaken, Switzerland, 14-19 September.

Nichols, A.L. and J.K. Tuli (2007), "The aims and activities of the International Network of Nuclear Structure and Decay Data Evaluators", *Proceedings of the International Conference on Nuclear Data for Science and Technology 2007*, 1, pp. 37, DOI:10.1051/ndata:07149.

Otsuka, N. (2014), "Towards a more complete and accurate experimental nuclear reaction data library (EXFOR: International Collaboration between Nuclear Reaction Data Centres (NRDC)", *Nuclear Data Sheets*, 120, pp. 272-276, DOI:10.1016/j.nds.2014.07.065.

Ravaux, S., D. Bernard and A. Santamarina (2013), "New evaluation of photon production for JEFF-3", *EPJ Web of Conferences 42*, 04002, DOI:10.1051/epjconf/20134204002.

Ravaux, S. (2014), "Qualification du Calcul de l'Echauffement Photonique dans les Réacteurs Nucléaires", PhD Thesis, Université de Grenoble, France, https://tel.archives-ouvertes.fr/tel-00961188.

Sheets, S.A., U. Agvaanluvsan, M. Krtička, G. E. Mitchell, J.A. Becker and F. Becvar (2006), "The radiative strength function using the neutron-capture reaction on $^{94,95}$Mo", *12th International Symposium on Capture Gamma-Ray Spectroscopy and Related Topics*, 4-9 September 2005, Notre Dame, Indiana, AIP Conference Proceedings 819, pp. 597-598, DOI:10.1063/1.2187935.

Sheets, S.A. et al. (2007), "Spin and parity assignments for $^{94,95}$Mo neutron resonances", *Physical Review C*, 76, 064317, DOI:10.1103/PhysRevC.76.064317.

Soppera, N., M. Bossant and E. Dupont (2014), "JANIS 4: An improved version of the NEA Java-based nuclear data information system", *Nuclear Data Sheets*, 120, pp. 294-296, DOI:10.1016/j.nds.2014.07.071.

Tuli, J.K. (1983), *Thermal Neutron Capture Gamma-Rays*, BNL-NCS-51647, Brookhaven National Laboratory, United States, DOI:10.2172/6236163.

Vaglio-Gaudard, C., A. Santamarina, P. Blaise, O. Litaize, A. Lyoussi, G. Noguère, J.M. Ruggieri and J.F. Vidal (2010), "Interpretation of PERLE experiment for the validation of iron nuclear data using Monte Carlo calculations", *Nuclear Science and Engineering* 166, 2, pp. 89-106, DOI: 10.13182/NSE09-91.

Webster, E.B. (1995), *WIMS Library: Selection of Fission Products for the WIMS 1995 Cross Section Library*, AEA-TSD-0347, AEA-Technology, United Kingdom.